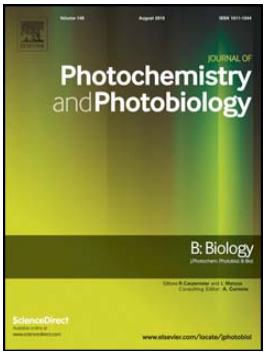

Design, synthesis, anticancer, antimicrobial activities and molecular docking studies of novel quinoline bearing dihydropyridines

S'busiso Mfan'vele Nkosi, Krishnan Anand, Srinivasan Anandakumar, Sanil Singh, Anil Amichund Chuturgoon, Robert Moonsamy Gengan

PII: S1011-1344(16)30751-5
DOI: doi:10.1016/j.jphotobiol.2016.10.009
Reference: JPB 10608

To appear in:

Received date: 1 September 2016
Revised date: 3 October 2016
Accepted date: 11 October 2016

Please cite this article as: S'busiso Mfan'vele Nkosi, Krishnan Anand, Srinivasan Anandakumar, Sanil Singh, Anil Amichund Chuturgoon, Robert Moonsamy Gengan, Design, synthesis, anticancer, antimicrobial activities and molecular docking studies of novel quinoline bearing dihydropyridines, (2016), doi:10.1016/j.jphotobiol.2016.10.009

Design, synthesis, anticancer, antimicrobial activities and molecular docking studies of novel quinoline bearing dihydropyridines

S'busiso Mfan'vele Nkosi[1], Krishnan Anand[1], Srinivasan Anandakumar[2], Sanil Singh[3], Anil Amichund Chuturgoon[4], Robert Moonsamy Gengan[1*]

[1]Department of Chemistry, Faculty of Applied Science, Durban University of Technology, Durban 4001, South Africa

[2]Department of Bioinformatics, School of life Sciences, Bharathiyar University, Coimbatore 641046, India

[3]Department of Biomedical Resource Centre, University of KwaZulu-Natal, Westville, Durban 4001, South Africa.

[4]Discipline of Medical Biochemistry, School of Laboratory Medicine and Medical Sciences, University of KwaZulu-Natal, Durban 4001, South Africa.

* Corresponding authors. E-mail address: genganrm@dut.ac.za

Abstract

A new series of eight quinoline bearing dihydropyridine derivatives (**A1-A8**) were synthesized in high yield and in short reaction time by a four component reaction of 2-chloro-3-fomyl quinoline, malononitrile, arylamines and dimethyl acetylenedicarboxylate in the presence of a catalytic amount of triethylamine. The compounds were fully characterised by IR, NMR and GC-MS. These compounds were screened for potential biological activity in an A549 lung cancer cell line and were also evaluated for their antibacterial activities against *Pseudomonas aeruginosa* ATCC 27853, *Escherichia coli* ATCC 25922 and *Staphylococcus aureus* ATCC 29213 whilst their molecular docking properties in an enzymatic system were also determined. Compounds A2, A3, A4 and A8 showed anti-proliferative activity; with A4 having the highest toxicity at 250 µg/mL and A8 has high toxicity at 125, 250 and 500 µg/mL, respectively. Antibacterial results indicated that A4 have significant activity against tested microorganisms at the minimum inhibitory concentration (MIC) values of 32 µg/mL against *Pseudomonas aeruginosa* and *Escherichia coli,* and 16 µg/mL against *Staphylococcus aureus*. Docking of **A1** with Human mdm2 indicated the lowest binding energy (-6.111 Kcal/mol) thereby showing strong affinity of the ligand molecule with the receptor which has been stabilized by strong hydrogen bond interactions in the binding pocket. This confirms that **A1** is a better inhibitor for E3 ubiquitin-protein ligase mdm2.

Keywords: 2-chloro-3-formylquinoline; dihydropyridines; molecular docking; anti-cancer; human mdm2

Introduction

Quinolines and their derivatives represent an important class of nitrogen-containing heterocycles as they are useful dyes and intermediates in organic synthesis (Heravi *et al*., 2007). In recent years, much attention has been focused on their synthesis as they possess useful biological activities such as anti-malarial (Golden *et al*., 2015), anti-inflammatory (Liu *et al*., 2015), bactericidal (Maddela *et al*., 2014), fungicidal (Nadaraj *et al*., 2012) and anti-cancer (Wu *et al*, 2003). Because of their important role in the pharmaceutical field (Litvinov *et al*., 2004), the profiles of quinolines and their pharmaceutical properties are well documented (Chipeleni *et al*., 2007; Kumar *et al*., 2009).

On the other hand, many naturally occurring and synthetic compounds bearing pyridine scaffold possess interesting biological properties (Temple *et al*., 1992) and they are well known for their versatile biological activities like antimicrobial (Mahmoud *et al*., 2007), antitubercular (Ashrafali *et al*., 2010; Lourenco *et al*., 2007), anticancer (Kawase *et al*., 2002) and antitumor activity (Safak *et al*., 2007). The polysubstituted pyridine represent molecular framework that serves as a platform for development of pharmaceutical agents. Thus, the synthetic of highly functionalized pyridine derivatives has become an active area of research (Anabha *et al*., 2007; Fletcher *et al*., 2006; Sridhar *et al*., 2009; Shinde *et al*., 2010). Encouraged by quinolines and pyridines potent clinical applications and in continuation of our previous investigations on biopotent heterocycles (Gengan *et al*., 2010, 2015) in this study, our efforts focused on the design and synthesis of more biological potent heterocyclic systems via combination of both therapeutically active moieties of quinoline and pyridine in a single scaffold.

Tandem multi-component reactions, in which multiple reactions are simulated in one synthetic operation, have been used comprehensively to form carbon-carbon bonds (Taylor *et al*., 2005). Such reactions offer a wide range of possibilities for the efficient formation of highly complex molecules in a single operation. Multi-component reactions (MCRs) are reactions using more than two starting materials that form a product which contains the key parts of all of the starting materials (Sinha *et al*., 2013) in a few *in-situ* reaction steps. Compared with conventional organic reactions, MCRs are more profitable and requires minimum energy to complete the reaction. Several MCRs are known which include the Ugi 4 component condensation of amine, ketone, carboxylic acid and isocyanide (Ugi *et al*., 1962).

The Strecker reaction, documented in 1850, was the first MCR described (Degussa *et al.*, 2003). Recently, there has been a tremendous development in three and four-component reactions and huge attempts have been made are continuously being made to discover and amplify new MCRs. Therefore, the development of new synthetic approaches using MCRs remains an active research area of study (Shestopalov *et al*., 2002). The literature reveals that quinoline bearing dihydropyridine derivatives in **Figure 1** have received much interest in the field of chemistry owing to their association with a variety of biological activities; (Yan *et al*., 2010; Nirmal *et al*, 2009; Ladani *et al*, 2011)

Cancer, a worldwide epidemic and one of the leading causes of death in developed countries, is responsible for 20-25% of all deaths (Bepler *et al*., 2007, El-Hussein *et al*., 2016). Lung cancer in humans is common and often fatal (Mehrotra *et al*., 2010). Quinolines play a significant role in the development of new anti-cancer agents; their derivatives have shown excellent results through different mechanism of action such as growth inhibitors by cell cycle arrest, apoptosis, inhibition of angiogenesis, disruption of cell migration, and modulation of nuclear receptor responsiveness (Firestone *et al*., 2009).

A number of developments have advanced drug discovery (Shoichet *et al*., 2002, Singh *et. al*., 2013). Increasingly, as the structures of more potential compounds are becoming available, molecular docking is progressively being studied for pharmacologically or biologically active chemical compounds (Clauben *et al*., 2001). Docking is a method which predicts the preferred orientation of one molecule to a moment when they bound to each other to form a stable complex. Docking it is a key tool in structural molecular biology and computer-assisted drug design. The goal of ligand-protein docking is to predict the predominant binding mode of a ligand with a protein of known three-dimensional structure (Kharb *et al*., 2011).

Pathogenic bacteria are becoming resistance to anti-microbial treatment because of acquired resistance genes in the DNA of the micro-organism. Therefore, the antibiotic resistance problem demands continuous discovery and development of new antibacterial agents that could be used for the effective treatment of infectious diseases (Gandhi and Khan *et. al*., 2016). Realizing the medicinal importance of quinoline and pyridine based compounds; we undertook an investigation to synthesize novel quinoline bearing dihydropyridine derivatives and study their application in biological systems. The scope of this study was to synthesize novel quinoline bearing dihydropyridine type molecules from simple and cost effective starting materials, hence, purify the compounds by chromatographic

techniques and characterize them by spectroscopy. Furthermore, the study seeks to also, assess and compare their potential as anti-cancer drugs in A549 lung cancer cell lines, evaluate their molecular modeling properties and anti-microbial activities.

Materials and Methods

Chemistry

All reagents and solvents such as aniline, *m*-toluidine, *o*-anisidine, fluoroaniline, chloroaniline, petroleum ether, ethanol, ethyl acetate and triethylamine were purchased from Lasec S.A, Aldrich, Fluka and Merck. These reagents and solvents were used without further purification. Melting points were recorded on Stuart Digital melting point apparatus. The ^{1}H and ^{13}C NMR, ^{19}F NMR, COSY, NOESY, HSQC and HMBC spectra were recorded either on Bruker (600 MHz) or Bruker (400 MHz) spectrophotometers in $CDCl_3$ or DMSO using tetramethylsilane (TMS) as an internal reference. The chemical shifts were quoted in parts per million (ppm). The IR spectra were recorded on Perkin Elmer 537 spectrophotometer and Shimadzu-8201 FT instrument, using ATR. Lung cancer cells (A549) were purchased from Highveld Biologicals (Johannesburg, SA). Cell culture reagents were purchased from Whitehead Scientific (Johannesburg, SA). Fresh Nutrient Agar, Oxoid LTD was purchased from Hamsphire, England and Fresh Mueller Hinton Broth from Sigma-Aldrich, (SA) all other reagents and consumables were purchased from Merck (SA), unless otherwise stated.

Synthesis of a starting compound 2-chloro-3-formyl quinoline

Dry DMF (3 mmol) was cooled to $0^{\circ}C$ in a flask equipped with a drying tube and then $POCl_3$ (12 mmol) was added drop-wise with stirring. To this solution, acetanilide (1 mmol) was added in small portions and after 25-30 minutes the reaction mixture was heated for 24 hours on a boiling water bath. The reaction mixture was poured into ice water and stirred for 30 minutes. The work-up was performed with aqueous NaOH to form a precipitate, to hydrolyse the imine salt and remove any acid formed. The solid was filtered, dried and purified from ethyl acetate to give 2-chloro-3-formyl quinoline in high yield (90 %).

General procedure for synthesis of quinoline bearing dihydropyridine derivatives (A1-A8)

In a round bottom flask, a mixture of 2-chloro-3-formyl quinoline (2.0 mmol, 0.3831g), malononitrile (2.0 mmol, 0.1324g) and triethylamine (1.0 ml) in 20 mL ethanol

was stirred at room for thirty minutes. Then a solution of arylamines (2.0 mmol) and dimethyl acetylenedicarboxylate (2.0 mmol, 0.284g) in 25.0mL ethanol was added to it. The solution was stirred at room temperature for ten hours. The resultant precipitate was collected by filtration and washed with cold ethanol to give the pure product and purified by column chromatography (50:50 Petroleum ether: Ethyl acetate).

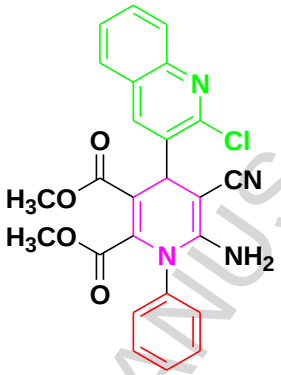

Dimethyl-6-amino-4-(2-chloroquinolin-3-yl)-5-cyano-1-phenyl-1,4-dihydropyridine-2,3-dicarboxylate **(A1):** Light yellow solid, 87%, m.p. 275-276^{0}C, ^{1}H NMR (600MHz, $CDCl_3$) δ: 8.14 (s, 1H, ArH), 8.02 (d, *J*= 8.4Hz, 1H, ArH), 7.84 (d, *J*= 8.1Hz, 1H, ArH), 7.71 (t, *J*= 7.3Hz, 2H, ArH), 7.55 (t, *J*= 7.6Hz ,1H, ArH), 7.52-7.51 (m, 2H, ArH), 7.39-7.38 (m, *2*H, ArH), 5.36 (s, 1H, CH), 4.13 (s, 2H, NH_2), 3.51 (s, 3H, OCH_3), 3.44 (s, 3H, OCH_3); ^{13}C NMR (600MHz, $CDCl_3$) δ: 165.28, 163.20, 150.22, 149.88, 146.93, 142.99, 138.59, 136.14, 134.89, 130.81, 130.47, 130.37, 130.09, 128.34, 127.62, 127.55, 127.11, 119.74, 103.55, 61.22, 52.66, 52.12, 36.94; (IR) υ/cm^{-1}: 3486, 3356, 2171, 1748, 1713, 1647, 1524, 1488, 1448, 1324, 1296, 1247, 1105, 1024, 992, 841, 835, 778, 762, 669, 667, 550. MS (*m/z*): 475. Anal Calculated for $C_{25}H_{19}ClN_4O_4$: C 63.23; H 4.03; Cl 7.47; N 11.80; O 13.48: Found, C 63.87; H 4.05; Cl 7.50; N 11.88; O 13.81.

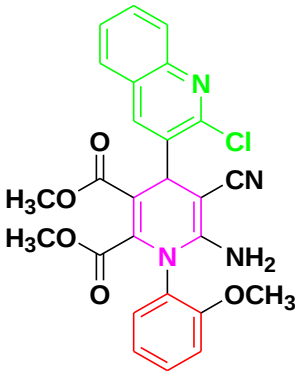

Dimethyl-6-amino-4-(2-chloroquinolin-3-yl)-5-cyano-1-(2-methoxyphenyl)-1,4-dihydropyridine-2,3-dicarboxylate **(A2):** Yellow solid, 40%, m.p. 263-264^{0}C, ^{1}H NMR (600MHz, $CDCl_3$) δ: 8.39 (s, 1H, ArH), 8.01 (d, *J*= 8.4Hz, 1H, ArH), 7.84 (d, *J*= 8.1Hz, 1H,

ArH), 7.80 (d, *J*= 8.1Hz, 1H, ArH) 7.69 (t, *J*= 7.6Hz, 1H, ArH), 7.53 (d, *J*= 7.1Hz, 1H. ArH), 7.49 (d, *J*= 7.8Hz, 1H, ArH), 7.30 (d, *J*= 7.3Hz, 1H, ArH), 7.06-7.02 (m, 1H, ArH), 5.36 (s, 1H, CH), 4.17 (s, 2H, NH_2), 3.50 (s, 3H, OCH_3), 3.49 (s, 3H, OCH_3), 3.46 (s, 3H, OCH_3); ^{13}C NMR (600MHz, $CDCl_3$) δ: 165.39, 163.33, 157.37, 150.89, 149.91, 146.91, 138.66, 132.57, 130.38, 128.53, 128.31, 127.56, 127.31, 127.03, 121.14, 121.04, 119.99, 112.7, 112.63, 61.80, 52.66, 52.54, 52,10, 36.36; (IR) υ/cm^{-1}: 3437, 3315, 3217, 2185, 1716, 1746, 1665, 1577, 1496, 1421, 1354, 1329, 1222, 1117, 933, 932, 859, 817, 782, 755, 624; MS (*m/z*): 504. Anal Calculated for $C_{26}H_{21}ClN_4O_5$: C 61.85; H 4.19; Cl 7.02; N 11.10; O 15.84: Found, C 61.87; H 4.25; Cl 7.10; N 11.08; O 15.81.

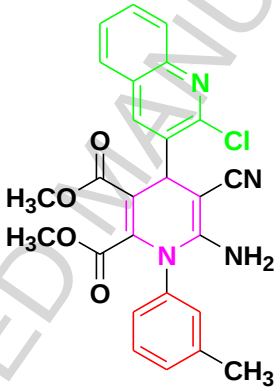

Dimethyl-6-amino-4-(2-chloroquinolin-3-yl)-5-cyano-1-m-tolyl-1,4-dihydropyridine-2,3-dicarboxylate **(A3):** Yellow solid, 73%, m.p. 237-238^{0}C, ^1H NMR (600MHz, $CDCl_3$) δ: 8.12 (s, 1H, ArH), 8.00 (d, *J*= 9.7Hz, 1H, ArH), 7.84 (d, *J*= 8.1Hz, 1H, ArH), 7.69 (t, *J*= 10.1Hz, 1H, ArH), 7.53 (t, *J*= 11.2Hz, 1H, ArH), 7.36 (t, *J*= 9.9Hz, 1H, ArH), 7.29 (d, *J*= 7.6Hz, 1H, ArH), 7.23 (s, 1H, ArH), 7.16 (d, *J*= 6.4Hz, 1H, ArH), 5.33 (s, 1H, CH), 4.23 (s, 2H, NH_2), 3.50 (s, 3H, OCH_3), 3.44 (s, 3H, OCH_3), 2.39 (s, 3H, CH_3). ^{13}C NMR (600MHz, $CDCl_3$) δ: 165.31, 163.20, 150.41, 149.87, 146.89, 143.06, 140.45, 138.53, 136.47, 134.74, 131.51, 130.70, 130.42, 129.79, 128.30, 127.67, 127.55, 127.15, 127.08, 119.91, 60.83, 52.61, 52.07, 36.73, 21.23; (IR) υ/cm^{-1}: 3386, 3318, 2180, 1702, 1647, 1565, 1488, 1420, 1358, 1328, 1253, 1224, 1136, 1114, 1056, 1019, 968, 928, 786, 763, 708, 686; MS (*m/z*) 487. Anal Calculated for $C_{26}H_{21}ClN_4O_4$: C 63.87; H 4.33; Cl 7.25; N 11.46; O 13.09: Found, C 63.20; H 4.31; Cl 7.11; N 11.36; O 13.23.

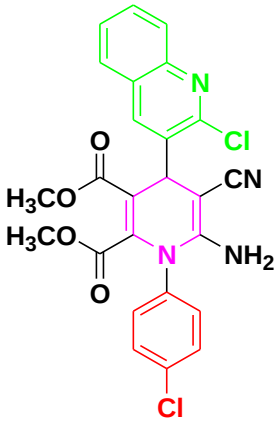

Dimethyl-6-amino-1-(4-chlorophenyl)-4-(2-chloroquinolin-3-yl)-5-cyano-1,4-dihydropyridine-2,3-dicarboxylate **(A4):** Light yellow solid, 79%, m.p. 287-289^{0}C, ^{1}H NMR (600MHz, DMSO) δ: 8.38 (s, 1H, ArH), 8.17 (d, *J*= 8.1Hz, 1H, ArH), 7.98 (d, *J*= 8.5Hz, 1H, ArH), 7.84 (t, *J*= 6.9Hz, 1H, ArH), 7.70 (t, *J*= 7.9Hz, 1H, ArH), 7.60 (d, *J*= 8.8Hz, 2H, ArH), 7.49 (d, *J*= 11.2Hz, 2H, ArH), 5.86 (s, 2H, NH_2), 5.24 (s, 1H, CH), 3.45(s, 3H, OCH_3), 3.43(s, 3H, OCH_3).^{13}C NMR (600MHz, DMSO) δ: 165.21, 163.13, 151.42, 149.57, 146.54, 143.31, 139.11, 137.73, 135.37, 134.41, 132.98, 131.37, 130.17, 128.52, 128.01, 127.92, 127.89, 127.87, 120.77, 103.14, 58.54, 52.43, 52.01, 39.60; (IR) υ/cm^{-1}: 3428, 3218, 2174, 1745, 1703, 1650, 1623, 1593, 1571, 1489, 1354, 1257, 1219, 1107, 1090, 1018, 850, 825, 780, 741, 723; MS (*m/z*) 510. Anal Calculated for $C_{25}H_{18}Cl_2N_4O_4$: C 58.95; H 3.56; Cl 13.92; N 11.00; O 12.56: Found, C 63.19; H 3.55; Cl 7.15; N 11.39; O 13.22.

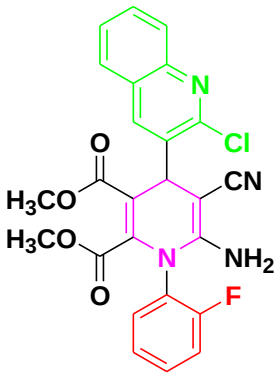

Dimethyl-6-amino-4-(2-chloroquinolin-3-yl)-5-cyano-1-(2-fluorophenyl)-1,4-dihydropyridine-2,3-dicarboxylate (**A5**): White solid, 64%, m.p. 247-248^{0}C, ^{1}H NMR (600MHz, DMSO) δ: 8.33 (s, 1H, ArH), 7.84 (d, *J*= 7.3Hz, 2H, ArH), 7.67 (d, *J*= 7.1Hz, 2H, ArH), 7.59 (m, 2H, ArH), 7.37-7.33 (m, 2H, ArH), 5.99 (s, 2H, NH_2), 5.22 (s, 1H, CH), 3.46 (s, 6H, OCH_3). ^{13}C NMR (600MHz, DMSO) δ: 165.59, 165.02, 164.10, 163.04, 160.57, 158.91, 151.33, 146.57, 143.21, 133.50, 133.44, 131.46, 129.07, 128.89, 128.66, 128.40,

128.07, 120.59, 79.62, 53.61, 53.15, 49.07, 40.53, 39.57, 29.44; (IR) υ/cm^{-1}: 3376, 3282, 2178, 1747, 1712, 1654, 1571, 1488, 1422, 1360, 1329, 1258, 1231, 1171, 1032, 967, 922, 872, 851, 761, 648, 644.

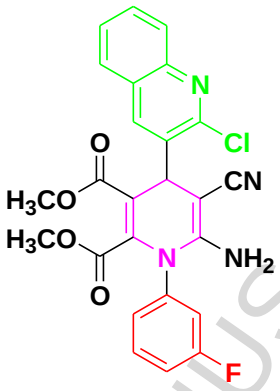

Dimethyl-6-amino-4-(2-chloroquinolin-3-yl)-5-cyano-1-(3-fluorophenyl)-1,4-dihydropyridine-2,3-dicarboxylate **(A6):** White solid, 31%, m.p. 269-271^{0}C, ^{1}H NMR (600MHz, DMSO) δ: 8.40 (s, 1H, ArH), 8.19 (d, *J*= 8.4Hz, 1H, ArH), 7.99 (d, *J*= 8.5Hz, 1H, ArH), 7.84 (t, *J*= 7.0Hz, 1H, ArH), 7.70 (t, *J*= 6.9Hz, 1H, ArH), 7.61-7.56 (m, 1H, ArH), 7.42 (m, 1H, ArH), 7.31 (d, *J*= 7.2Hz, 1H, ArH), 5.86 (s, 2H, NH_2), 5.25 (s, 1H, CH), 3.45 (m, 3H, OCH_3), 3.40 (m, 3H, OCH_3), ^{13}C NMR (600MHz, DMSO) δ: 165.75, 163.09, 161.65, 151.60, 149.57, 145.55, 143.15, 139.12, 137.87, 136.84, 131.61, 131.56, 131.36, 128.55, 128.00, 127.74, 120.74, 121.91, 118.74, 117.86, 58.75, 52.96, 52.09, 37.10; (IR) υ/cm^{-1}: 3449, 3303, 2177, 1746, 1715, 1652, 1596, 1570, 1487, 1421, 1329, 1305, 1251, 1194, 1136, 1106, 1033, 966, 924, 819, 763, 706, 899. ^{19}F NMR (600MHz, DMSO) δ: 111.23; MS (*m/z*) 494. Anal Calculated for $C_{25}H_{18}ClFN_4O_4$: C 60.92; H 3.68; Cl 7.19; F 3.85; N 11.37; O 12.98: Found, C 60.90; H 3.68; Cl 7.11; F 3.84; N 11.36; O 12.99.

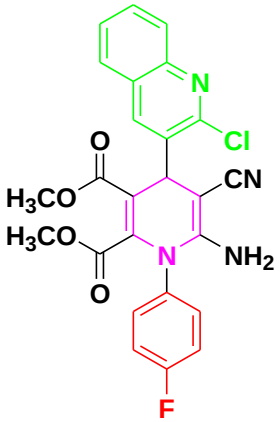

Dimethyl-6-amino-4-(2-chloroquinolin-3-yl)-5-cyano-1-(4-fluorophenyl)-1,4-dihydropyridine-2,3-dicarboxylate **(A7):** White solid, 60%, m.p. 253-254^{0}C, ^{1}H NMR

(600MHz, DMSO) δ: 8.38 (s, 1H, ArH), 8,17 (d, *J*= 8.0Hz, 1H, ArH), 7.96 (d, *J*= 7.6Hz, 1H, ArH), 7.82 (t, *J*= 7.3Hz, 1H, ArH), 7.66 (t, *J*= 7.2Hz, 1H, ArH), 7.54-7.52 (m, 2H, ArH), 7.38-7.34 (m, 2H, ArH), 5.83 (s, 2H, NH_2), 5.23 (s, 1H, CH), 3.43 (s, 3H, OCH_3) 3.38 (s, 3H, OCH_3); ^{13}C NMR (600MHz, DMSO) δ: 150.99, 149.9, 149.14, 145.99, 143.03, 142.97, 138.60, 137.44, 137.34, 133.38, 133.37, 133.34, 133.33, 133.26, 113.1.1, 130.06, 128.00, 127.95, 127.38, 120.37, 116.32, 61.65, 57.83, 57.32, 36.77; (IR) υ/cm^{-1}: 3309, 3269, 2171, 1745, 1702, 1622, 1506, 1569, 1329, 1298, 1247, 1213, 1153, 1106, 1027, 1002, 938, 918, 840, 778, 768, 766, 741, 728, 615. ^{19}F NMR (600MHz, DMSO) δ: 110.91; MS (*m/z*) 494. Anal Calculated for $C_{25}H_{18}ClFN_4O_4$: C 60.92; H 3.68; Cl 7.19; F 3.85; N 11.37; O 12.98: Found, C 60.90; H 3.68; Cl 7.11; F 3.84; N 11.38; O 12.97.

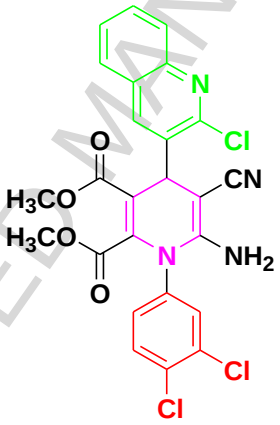

Dimethyl-6-amino-4-(2-chloroquinolin-3-yl)-5-cyano-1-(3,4-dichlorophenyl)-1,4-dihydropyridine-2,3-dicarboxylate **(A8):** Light yellow solid, 72%, m.p. 280-282^{0}C, ^1H NMR (600MHz, DMSO) δ: 8.45 (s, 1H, ArH), 8.20 (d, *J*= 8.1Hz, 1H, ArH), 7.99 (d, *J*= 8.4Hz, 1H, ArH), 7.85 (d, *J*= 7.7Hz, 1H, ArH), 7.84 (t, *J*= 7.7Hz, 1H, ArH), 7.70 (t, *J*= 7.6Hz, 1H, ArH), 7.48 (d, *J*= 2.2Hz, 1H, ArH), 7.47 (d, *J*= 2.3Hz, 1H, ArH), 6.02 (s, 2H, NH_2), 5.25 (s, 1H, CH), 3.43 (s, 3H, OCH_3), 3.39 (s, 3H, OCH_3); ^{13}C NMR (600MHz, DMSO) δ: 165.20, 163.10, 151.14, 149.58, 146.54, 142.88, 139.38, 137.78, 135.36, 133.79, 133.53, 132.33, 131.79, 131.55, 131.34, 130.17, 128.54, 127.96, 127.84, 120.73, 79.65, 53.09, 53.00, 39.60; (IR) υ/cm^{-1}: 3439, 3302, 2179, 1742, 1702, 1647, 1573, 1506, 1423, 1366, 1324, 1254, 1214, 1108, 1032, 932, 758; MS (*m/z*) 544. Anal Calculated for $C_{25}H_{17}Cl_3N_4O_4$: C 55.22; H 3.15; Cl 19.56; N 10.30; O 11.77: Found, C 65.19; H 3.16; Cl 19.15; N 10.39; O 11.22.

Anticancer study

Maintenance of A549 Cells in Culture

The best environment for growing cells *in vitro* should be matched as close as possible to the natural physiological conditions. The essential requirements are an environment of optimum temperature, pH, gas phases, growth substrate and media containing necessary nutrients. The optimal temperature is provided by the use of a humidified incubator supplied with 5% CO_2. The gas phases supplied to the culture includes oxygen which is maintained at atmospheric pressure, and CO_2 to ensure that the bicarbonate and CO_2 tension is in equilibrium. A549 cells were cultured (37^0C, 5% CO_2) to 90% confluency in 25mL flasks in complete culture media (CCM) [Eagle's minimum essential medium, 10% foetal calf serum, 1% L-Glutamine and 1% penstrepfungizone]. The culture medium is by far the most important single factor in culturing cells. The extracellular medium must meet the essential requirements (nutritional, hormonal and stromal factors) for survival and growth.

Trypsinisation

In order to sub-culture and plate cells for the various experimental assays, the process of trypsinisation was used to detach cells once 90% confluency was reached. The process of trypsinisation involved the critical step of rinsing the cells with 3 mL aliquots of warm 0.1M PBS and incubating the cells with 1 mL of trypsin-EDTA (Lonza) for 1 minute. The cells were monitored using an inverted light microscope (Olympus IXSI; 20x magnification) and once rounded, the trypsin was discarded and CCM was added to the flask of cells. The flask was agitated to detached cells and the cell suspension was then enumerated by dye exclusion using a haemocyto meter. Trypan blue (0.4%) was utilized in a dye exclusion procedure for cell counting. The principle of dye exclusion using trypan blue is based on compromised cell membranes in dead/damaged cells which readily allow entry of the dye into the cells and are stained blue whereas viable cells remain unstained.

Cell antiproliferation assay

The effect of newly synthesised compounds in A549 cells was measured using a methyl tetrazolium dye reduction assay, the [3,(4,5-dimethylthiazol-2-yl)-2,5-diphenyl tetrazolium bromide] (MTT) assay. This assay measures cell antiproliferative assay *in vitro*. This technique is particularly useful for cells that are metabolically active based on their redox potential and capacity of dehydrogenase enzymes to convert yellow water-soluble salt into a purple water-insoluble formazan product. The insoluble crystals are then dissolved in dimethyl sulfoxide (DMSO) and the absorbance is read on a spectrophotometer. The amount

of formazan produced is directly proportional to cell number thus allowing for the determination of cell viability and proliferation (Supino *et al*., 1995).

A549 cells (15,000/well) were incubated for 24 hours with a range of concentrations of each compound in triplicate in a micro-titre plate together with an untreated control (cells incubated with CCM only). Each experiment was conducted twice on separate occasions. The data results from the first set matched the repeated experiment. The cells were then incubated (37^0C, 5% CO_2) with the MTT substrate (5 mg/mL in PBS) for 4 hours. Thereafter all supernatants were aspirated, and DMSO (100 µl/well) was added to the wells. Finally the optical density was measured at 570 nm and a reference wavelength of 690 nm with an ELISA plate reader (Bio-Tek µQuant).

Antibacterial study

Preparation of Media and Nutrient Broth

Fresh Nutrient Agar and Fresh Mueller Hinton Broth were prepared according to the manufacturer's instructions. The cultures of *Staphylococcus aureus, Escheriachia coli* and *Pseudomonas aeuginosa* were maintained on nutrient agar slopes at 4°C and sub cultured on to blood agar plates for 24 hours before use.

Microplate Alamar Blue Assay (MABA)

An amount of 0.2g of Resazurin powder was dissolved in 10 mL autoclaved distilled water. The dye solution was vortexed vigorously; the solution was immediately covered with aluminium foil to keep away from light as it is light sensitive.

The *in vitro* antibacterial activities of the synthesized compounds were studied by MABA using 96-wells microplates. Bacterial cultures were diluted in broth to turbidity comparable to that of a 0.5 McFarland turbidity standard and 20 µL of each bacterial dilution was distributed in all 96 wells of microplate including positive control (containing standard antibiotic) and growth control (containing culture broth without testing materials). Then 20 µL of each concentration of the synthesized compounds were added to two neighbour wells except for positive and growth control wells.

After adding Alamar Blue (20 µL) to all of 96 wells, the total volume in each well reached 200 µL. The final concentrations of the tested compounds were 256, 128, 64, 32, 16, 8, 4, 2, 1 µg/mL etc. After incubation, results were recorded as MIC (minimum concentration of each synthesized compound which completely inhibited growth of microorganism). The

stock solutions of the synthesized compounds were prepared by dissolving in the minimum volume of DMSO.

Molecular Docking

The crystal structure of human mdm2 (**PDB ID: 3VZV**), were retrieved from the Protein Data Bank After selected the protein structure, protein preparation wizard of Schrodinger suite was used to prepare protein structure. All the water molecules were removed from the protein structure. Metal was treated and hydrogen atoms were added. All atom force field (**OPLS-2005**) charges and atom types were assigned. Protein structure energy was minimized. The chemical compounds structures were not available in pubchem database. Therefore, we used chem sketch to draw the compound structure. All the ligands were prepared for molecular docking studies using ligprep version 2.3 (Ligprep *et al*., 2009). The ligand structure energy was minimized; partial atomic charges were computed using the OPLS-2005 force field by using Schrödinger suite.

The prepared protein structure was followed up by the grid-fashion kinetic docking which commonly holds several physical parameters and finds greater significance in prescribing the ligand interaction with the receptor. Grid files generation for protein was accomplished with "Receptor Grid Generation" panel of Glide. The grid box was generated by assigning a common constituency point. From there an actually cubic grid box was extended to touch the bounty of 20Å in size. In other words, the allocated size for grid generation of protein-ligand docking was 20Å since our approach was site-specific not generalized. Having observed that co-crystal ligand binding pattern with protein is already well documented in recent studies, we attempted to crop the grid box to focus on the centroid of human mdm2 refined structure and box coordinate X, Y, Z were set at (X=18.341215Å, Y=-3.662453Å, Z=0.929674Å). The foremost process in the hit identification pipeline, docking is performed using Glide of Schrodinger (Glide *et al*., 2009).

Results and Discussion

The focus of this research was to synthesize novel compounds, especially compounds that contain functional groups with potential biological activities. Since heterocycles containing quinoline are reported to improve the biological activity of organic compounds, our aim was to synthesize novel quinolone bearing dihydropyridine derivatives. Also, we decided to use MCR, therefore, our first objective was to synthesize a formyl quinoline

derivative using Vilsmeier-Haack reaction (Srivastava *et al*., 2005) which could be used as one of the substrates for the one pot MCR.

Scheme 1: Synthesis of quinoline bearing dihydropyridines

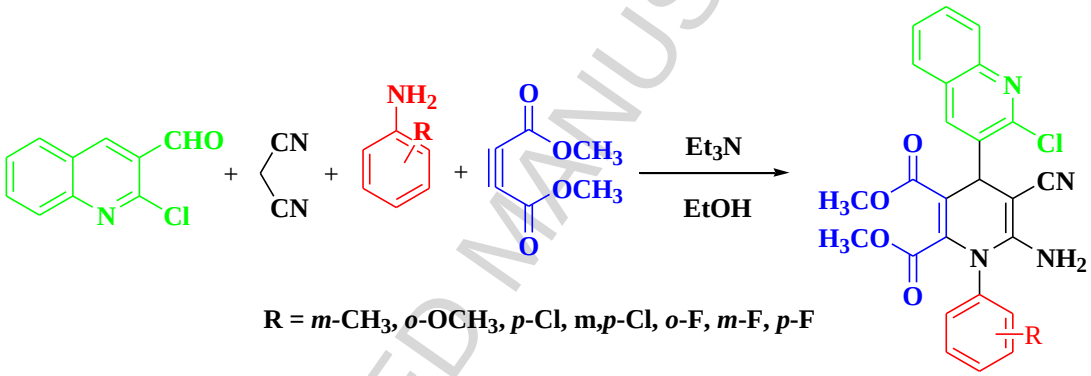

R = *m*-CH_3, *o*-OCH_3, *p*-Cl, m,*p*-Cl, *o*-F, *m*-F, *p*-F

Table 1: Synthesis of quinoline bearing dihydropyridines derivatives

Entry	Compound	Ar	% Yield	Mp (°C)
1	A1	C_6H_4	87	275~276
2	A2	*o*-$OCH_3C_6H_4$	40	263~264
3	A3	*m*-CH_3-C_6H_4	73	237~238
4	A4	*p*-ClC_6H_4	79	287~288
5	A5	*o*-FC6H4	64	247~248
6	A6	*m*-FC6H4	31	269~271
7	A7	*p*-FC6H4	60	253~254
8	A8	*m,p*-ClC6H4	72	280~282

The identity of all the compounds (**A1- A8**) were confirmed by analysing the spectral data obtained from IR, ^{1}H NMR, ^{13}C NMR and GCMS. All the spectra were well resolved. We selected **A1** as the template and characterised the structure fully with the aid of 2D NMR techniques especially HSQC, HMBC, COSY and NOESY which led to the unambiguous assigning of all protons and carbons. We used the characterization of **A1** as a template to elucidate the other 7 derivatives. The IR spectra of **A1** showed the C=O stretching at 1713

cm^{-1} and 1748 cm^{-1}, the C-N stretching at 2171 cm^{-1}, the C-Cl stretching at 669-778 cm^{-1} whilst the NH stretching at 3486 cm^{-1} and 3356 cm^{-1} was not well resolved.

The ^{1}H NMR spectrum of **A1** showed singlets at δ 3.44 and δ 3.51 for two acetoxy groups (H-9', H-10'). The singlets at δ 4.13 and δ 5.35 were assigned to the amino (NH_2) and aliphatic proton (H-4') on the dihydropyridine ring, respectively. The peaks at δ 8.14-7.38 were attributed to aromatic protons. The chemical shifts, spin multiplicities and coupling constants (in Hertz) were assigned as: δ 8.14 (H-4, s); δ 7.84 (d, H-6, 3.2); δ 7.71 (t, H-7, 7.6); δ 7.64 (t, H-8, 7.4); δ 8.02 (d, H-9, 8.4); δ 7. 39-7.36 (m, H-2", H-4", H-6"); δ 7.54-7.51 (m, H-3"-H-5"). The COSY spectrum, presented in **Figure S4**, shows H-9 has a strong coupling with H-8 but a weaker coupling with H-7. The corresponding carbon resonances of H-7, H-8 and H-9 appeared at δ 130.17, 130.87 and 130.47, respectively and the absence of correlation between the carbons to the amino protons confirm the assignment of the NH_2, according to the HSQC spectrum, presented in **Figure S6.** The NOESY spectrum, presented in **Figure S7**, shows the coupling of H-9 to H-8; H-6 is coupled to H-7 and H-8 whilst H-7 is coupled to H-6 and H-8. Furthermore, the COSY spectrum shows a strong coupling between H-6 and H-7 and between H-7 and H-8 whilst a weak coupling is observed between H-7 and H-9. Also H-4 lacked any coupling signals. Both H-4 and H-6 shows the HMBC correlations to C-2, C-4' and C-5, presented in **Figure S5,** at δ 150.99, 120.33 and 134.90, respectively. The ^{4}J correlations at H-4' to C-5 and H-4' to C-8, ^{5}J correlation at H-6 to C-4' were also observed. The H-6" proton resonance shows a COSY correlation to H-5" and was confirmed by HSQC correlations between C-6" and C-5" occurring at δ 128.00 and 127.49, respectively. **Figure 2** shows the HMBC correlation for **A1**.

The ^{13}C NMR spectrum of **A1** is presented in **Figure S8.** The peaks at δ 51.90 and δ 52.34 were assigned to the two acetoxy carbons (C-9', C-10'); the peak at δ 58.06 was assigned to carbon of CN (C-3') and the peak at δ 39.03 was assigned to the C-H (C-4') on the dihydropyridine ring. The peaks at δ 162.64 are assigned to the two C=O (C-7', C-8'); the peak at δ 164.73 was assigned to the C-NH_2 (C-2') whilst the peaks at δ 150.99-120.33 were attributed to aromatic carbons. The ^{13}C NMR spectra of all compounds were appropriate to their formulas. Mass spectra of the compounds showed m/z in accordance with their formulas. The mass spectrum of **A1** is presented in **Figure S9,** it shows the *m/z* value for the molecular ion corresponding to the proposed molecular formula at 475.

The cancer study was used to investigate the cytotoxicity of synthesized quinoline derivatives (**A1-A8**) in the A549 lung cancer cell line. These compounds differed in substituents like OCH_3, CH_3, F and Cl attached to the benzene ring. Herein we decided to

investigate the effect of these compounds based on the different functional groups to study their anticancer potential. At this stage of our investigation, we were unable to source out a suitable standard containing the dihydropyridine nucleus and hence we selected **A1** as a reference point. Our hypothesis was that the presence of functional groups present in the phenyl part will influence cytotoxicity. The parent compound **A1** (with no substituent in the benzene ring) is not cytotoxic but rather increases metabolic activity as all concentrations tested show greater activity than control. The compound **A2** (with an electron donating group, OCH_3 substituent in the benzene ring), shows a dose dependent toxicity due to its substituent as the results gives evidence that the compound has potential as an anti-cancer drug. The compound **A3** (with an electron donating group, CH_3 substituent in the benzene ring) shows high toxicity due to its CH_3 substituent but only at higher concentrations; has potential as an anti-cancer drug. The compound A4 (with the chloro group, which withdraws electrons by induction, but donates electrons by resonance in the benzene ring) showed a dose dependent toxicity with the highest toxicity at 250µM. The compound had potential as an anti-cancer drug. **A5**, **A6** and **A7** (with the fluoro group in the benzene ring) were not cytotoxic. A8 (with the two chloro groups, which withdrew electrons by induction, but donated electrons by resonance in the benzene ring) showed a dose dependent toxicity with the highest toxicity at 125, 250 and 500 µM. The compound had potential as an anti-cancer drug.

All Compounds (**A1-A8)** were evaluated for antibacterial activity against two Gram-negative bacteria, *E. coli* and *P. aeruginosa* and one Gram-positive bacterium, *S. aureus*. Standard antibiotics, ciprofloxacin and nalidixic acid were used as positive controls and DMSO used as negative control. DMSO had no effect on the bacteria in the concentrations. The antimicrobial activity results, **Table 3** revealed that the synthesized compounds showed moderate to good activity towards the mentioned panel of bacteria strains. It is interesting to note that compound with substituted anilines in the *para* position (**A4**, **A7** and **A8**) showed very good activity against all strains. These compounds were found more potent than both standards, ciprofloxacin (MIC = 50 µM) and nalidixic acid (MIC = 50 µM) towards *S. aureus* and *P. aeruginosa.* Compound **A1** (MIC = 128 µM) exhibited comparable activity as the standard nalidixic acid (MIC = 128 µM) against *P. aeruginosa* but showed no inhibitory effect against *S. aureus E. coli*. Compounds **A2** and **A3** showed poor activity towards all strains compared with the standard antibiotics.

Table 3: Antibacterial activities of (A1-A8): Minimum Inhibitory Concentration

Compound	*Staphylococcus aureus* (µM)	*Pseudomonas aeruginosa* (µM)	*Escherichia coli* (µM)
A1	-	128	256
A2	256	256	256
A3	256	256	256
A4	16	32	32
A5	128	256	128
A6	-	256	-
A7	32	32	32
A8	8	16	32
Nalidixic Acid	50	128	16
Ciprofloxacin	50	25	25
DMSO	-	-	-

The binding mode of **A1** within the active site of the human mdm2 was analyzed and the suitable shape of the compound helped it to bind tightly with the active site of the human mdm2. There was one hydrogen bond interaction formed between the side chains of the hydrophobic residue of TYR 104. The bond lengths between **A1** into the active site of the human mdm2 were observed (2.15Å). Docking of **A1** with Human mdm2 indicated lowest binding energy, glide score -6.111 Kcal/mol and glide energy -62.406 Kcal/mol thereby showing strong affinity of the ligand molecule with the receptor which had been stabilized by strong hydrogen bond interactions in the binding pocket. Furthermore, the following residues were mainly involved in hydrophobic interaction LEU27, VAL28, MET50, LEU54, PHE55, ILE61, MET62, TYR67, VAL75, VAL93, and ILE99. **Table 3** shows the docking results of all of the compounds **(A1-A8),** glide score (Kcal/mol), glide energy (Kcal/mol), interacting residues, distance between the protein and ligand (Å), hydrogen bond donor and hydrogen

bond acceptor. **Figure 11a, 11b, and 11c** shows hydrogen bond formation, hydrogen bond formation and bond length and the binding mode of **A1** compound with E3 ubiquitin-protein ligase mdm2.

Table 3: Glide extra-precision (XP) for (A1- A8) with human mdm2 by use of Schrodinger

Title	Glide Score	Glide energy	No. of H bonds	Interacting Residues	Distance (Å)	Hydrogen bond donor	Hydrogen bond acceptor
A1	-6.111	-62.406	1	Tyr 104	2.15	Ligand: (H)	A: TYR 104: (O)
A2	-2.616	-27.659	-	-	-	-	-
A3	-4.391	-35.217	1	Thr 26	2.04	A: THR 26: (H)	Ligand: (O)
A4	-3.963	-16.574	1	Thr 26	1.97	A: THR 26: (H)	Ligand: (O)
A5	-4.995	-44.146	1	Thr 26	2.05	A: THR 26: (H)HG1	Ligand: (O)
A6	-4.667	-42.032	1	Thr 26	2.04	A: THR 26: (H)HG1	Ligand: (O)
A7	-1.089	-19.121	4	Arg 29	1.93	A: ARG29: (H)HH21	Ligand: (N)
					2.25		Ligand: (N)
				Glu 25	2.25	B: LYS 51: (H)HZ1	Ligand: (H)
				GLY 25	2.46	A: GLY 25: (O)OE1	Ligand: (O)
						A: GLY 25: (H)H1	
A8	-3.497	-49.899	1	Thr 26	2.15	A: THR 26: (H)HG1	Ligand: (O)

Conclusion

All Compounds containing quinoline and dihydropyridine nucleus in a single molecular frame work were efficiently synthesized and fully characterized. *In vitro* anticancer and antibacterial studies were carried out; molecular docking was also investigated. The biological studies revealed that these compounds are selective in their action. The anti-cancer assay indicated that compounds **A2, A3, A4** and **A8** have good potential as an anticancer drug. The results obtained from the antibacterial assay showed that compounds A4, A7 and A8 have good activity compared to that of standard drugs, whereas **A2** and **A3** showed poor activity against the tested bacterial strains. Compound **A1** showed no inhibitory effect against *S. aureus E. coli*. Docking of **A1** with Human mdm2 indicated the lowest binding energy thereby

showing strong affinity of the ligand molecule with the receptor which has been stabilized by strong hydrogen bond interactions in the binding pocket. This confirms that **A1** is a better inhibitor for mdm2. Hence compound **A2-A8** showed an interesting correlation between docking scores and experimental binding data.

Acknowledgement

We are grateful to the National Research Foundation (NRF) and Durban University of Technology (DUT) for funding this project.

References

Anabha, E.R., Nirmala, K.N., Thomas, A., Asokan, C.V. 2007. Synthesis of 3-aroylnicotinonitriles from aroylketene dithioacetals. *Synthesis.* 3, 428-432.

Ashrafali, M., Shahar yar, M., Kumar, M., Pandian, G. 2010. Synthesis and antitubercular activity of substituted novel pyrazoline derivatives. *Nat. Prod. Res.* 21, 575-579.

Bepler. G. 2007. Preoperative Exercise Vo2 Measurement for lung resection candidates: results of cancer and leukemia group B protocol 9238. *J. Thoracic Oncology.* 2, 619-625.

Chipeleni, A., Gut, J., Rosenthal, P.J., Chibale, K. 2007. Synthesis and biological evaluation of phenolic Mannich bases of benzaldehyde and (thio) semicarbazone derivatives against the Cystein protease falcipain-2 and a chloroquine resistant strain of Plasmodium falciparum. *Biol. Med. Chem.* 15, 273-282.

Craig, J.C., Person, P.E. 1991. Potential anti-malarials, tribromomethylquinolines and positive halogen compounds. *J. Med. Chem.* 14, 1221-1222.

Clauben, H., Buninga, C., Rareya, M., Lengauera, T. 2001. Efficient molecular docking considering protein structure variations. *J Mol. Biol*. 308, 377-395.

Degussa, A.G. 2003. Catalytic enantioselective Strecker Reactions and analogous syntheses. *Chem. Rev*. 103, 2795-2827.

Dillard, R.D., Pravey, D.E., Benslay, D.N. 1973. Synthesis and anti-inflammatory activity of some 2,2-dimethyl-1,2-dihydroquinolines. *J. Med. Chem.* 16, 251-253.

El-Hussein, A. 2016. Study DNA damage after photodynamic therapy using silver nanoparticles with A549 cell line. *J. Nanomed. Nanotechnol.* 7, 346.

Firestone, G.L. 2009. Anticancer activities of artemisinin and its bioactive derivatives, *Rev. Mol. Med*. 1, 11.

Fletcher, M.D., Hurst, T.E., Miles, T.J., Moody, C.J. 2006. Synthesis of highly-functionalized pyridines via hetero-diels-alder methodology: reaction of 3-siloxy-1-aza-1,3-butadienes with electron deficient. *Tetrahedron.* 62, 5454-5463.

Gandhi. H., Khan, S. 2016. Biological synthesis of silver nanoparticles and its antibacterial activity. *J. Nanomed. Nanotechnol*. 7, 366.

Gengan, R.M., Pandian, P., Kumarsamy, C., Mohan, P.S. 2010. Convenient and efficient microwave-assisted synthesis of a methyl derivative of the fused indoloquinoline alkaloid cryptosanguinolentine, *Molecules. 15*, 3171-3178.

Golden., E.B., Cho H.Y., Hofman F.M., Louie S.G., Schönthal A.H., Chen T.C. 2015. Quinoline-based antimalarial drugs: a novel class of autophagy inhibitors. *Neurosurg Focus*. 3, 50.

Heravi, M.M., Tehrani, M.H., Bhakhtiari, K., Oskooie, H.A. 2007. Synthesis of 2,4,5-triaryl-imidazoles catalyzed by $NiCl_2{\cdot}6H_2O$ under heterogeneous system. *Catalysis Comm.* 8, 1341-1344.

Kharb, R., Shahar, Y.M. 2011. Recent advances and future perspectives of triazole analogs as promising antiviral agents, *Rev. in Med. Chem.* 11, 84-96.

Kawase, M., Shah, A., Gaveriya, H., Motohashi, N., Sakagami, H., Varga, A J. 2002. 3.5-Dibenzoyl-1.4-dihydropyridines; Synthesis and MDR reversal in tumor cells. *Bioorg. Med. Chem.* 10, 1051-1055.

Kumar, S., Bawa, S., Gupta, H. 2009. Biological activities of quinoline derivatives, *Mini Rev. Med. Chem*. 9, 1650-1654.

Ladani, N.K., Mungra, D.C., Patel, M.P., Patel, R.G. 2011. Microwave assisted synthesis of novel Hantzsch 1,4-dihydropyridines, acridine-1,8-diones and polyhydroquinolines bearing the tetrazolo[1,5-a]quinoline moiety and their antimicrobial activity assess, *Chinese Chem. Lett.* 22, 1407-1410.

Litvinov, V.P. 2004. Thienopyrimidines: synthesis, properties, and biological activity, *Russian Chem. Bulletin* 53, 487-516.

Liu, D., Wen, X., Wang, S. 2015. Synthesis and evaluation of the anti-inflammatory activity of quinoline derivatives. *Med. Chem. Res*. 24: 2591.

Lourenco, M.C.S., De Souza, M.V.N., Pinheiro A.C., Ferreira, M.L., Gonçalves R.S.B., Nogueira, T.C.M., Peralta M.A. (2007) Evaluation of anti-tubercular activity of nicotinic and Isoniazid. *Arkivoc.* 15, 181-191.

Maddela1., S., Ajitha., M., Venugopal., M., Maddela., R. 2014. Design and synthesis of novel quinoline 3-carbohydrazone derivatives for their antimicrobial and antioxidant activity. *Int. J. Pharmacy and Pharmaceutical Sciences*. 6, 254-258.

Mahmoud, M.R., El-Bordany, E.A.A., Hassan, N.F., Abu El-Azm F.S.M. 2007. Utility of nitriles in synthesis of pyrido[2,3-d]pyrimidines, thiazolo[3, 2-a]pyridines, pyrano[2,3-b]benzopyrrole, and pyrido[2,3-d]benzopyrroles. *Phosphorus Sulfur Silicon.* 182, 2507-2521.

Mehrotra, A., Nagarwal, R.C., Pandit, J.K. 2010. Fabrication of lomustine loaded chitosan nanoparticles by spray drying and in vitro cytostatic activity on human lung cancer cell line L132. *J. Nanomedic. Nanotechnolo.* 103, 2157-7439.

Nadaraj, V., Selvi, S.T. 2012. Synthesis and characterization of some quinoline bearing isoxazoles nucleus. *J. Chem. Pharm. Res.* 4, 2850-2853.

Nirmal J.P., Patel M.P., Patel R.G. 2009. Microwave-assisted synthesis of some new biquinoline compounds catalyzed by DMAP and their biological activities, *Indian J. Chem.* 48B, 712-717.

Pitchai, P., Sathiyasselan, M., Nepolraj, A., Gengan, R.M. 2015. An elegant synthesis of indoloquinoline alkaloid cryptotackieine via Vilsmeier-Haack approach. *Indian J. Chem.* 54, 1290-129.

Safak, C., Simsek, R. 2006. Fused 1,4-dihydropyridine as potential calcium modulatory compounds. *Mini. Rev. Med. Chem*. 6, 747-755.

Schrodinger, Glide, Version 5.5., 2009. LLC, New York, NY.

Schrodinger, Ligprep, Version 2.3., 2009. LLC, New York, NY.

Shinde, P.V., Sonar, S.S., Shingate, B.B., Shingare, M.S. 2010. Boric acid catalyzed convenient synthesis of 2-amino-3,5-dicarbonitrile-6-thio-pyridines in aqueous media. *Tetrahedron Lett.* 51, 1309-1312.

Singh, R., Wagh, P., Wadhwani, S., Gaidhani, S., Kumbhar, A., Bellare, J., Balu Ananda Chopade, B.A. 2013. Synthesis, optimization, and characterization of silver nanoparticles from acinetobacter calcoaceticus and their enhanced antibacterial activity when combined with antibiotics. *Int. J. Nanomedicine.* 8, 4277-4290.

Sinha, M.K., Khoury, K., Herdtweck, E., Domling, A. 2013. Tricycles by a new Ugi variation and Pictet-Spengler reaction in one pot. *Eur J. Chem.* 19, 8048-8052.

Shestopalov, A.M., Evans, D.H. 2002. One-step synthesis of substituted 6-Amino-5-cyanospiro-4-(piperidine-4')-2H, 4H-dihydropyrazolo [3,4-b]pyrans. *Org. Lett.* 16, 423-425.

Sun J., Xia, E., Wu, Q., Yan, C. 2010. Synthesis of polysubstituted dihydropyrdines by four-component reactions of aromatic aldehydes, malononitrile, arylamines and acetylenedicarboxylate *Org. Lett. 12* (16), 3678-3681.

Supino, R., MTT assays. 1995. *Methods Mol. Biol*. 43, 137.

Shoichet, K.B., McGovern, L.S. 2002. Molecular docking and high-throughput screening for novel inhibitors of protein tyrosine phosphatase-1B. *J. Med. Chem.* 45, 2213-2221.

Sridhar, M., Ramanaiah, B.C, Narsaiah, C., Mahesh, B., Kumaraswamy, M., Mallu, K.K.R., Ankathi, V.M., Rao P. 2009. Novel $ZnCl_2$-catalyzed one-pot multicomponent synthesis of 2-amino-3,5-dicarbonitrile-6-thio-pyridines. *Tetrahedron Lett.* 50, 3897-3900.

Srivastava, A., Singh, R.M. 2005. Vilsmeier-Haack reagent: A facile synthesis of 2-chloro-3-formylquinolines from N-arylacetamides and transformation into different functionalities, *Indian J. Chem*. 44, 1868.

Taylor, R.J.K., Reid, M., Foot, J., Raw, S.A. 2005. Organic Syntheses, *Collective. Acc. Chem. Res.* 12, 66-69.

Ugi, I. 1962. The solution phase synthesis of diketopiperazine libraries via the Ugi reaction: novel application of Armstrong's convertible isonitrile. *Angew. Chem. Int Ed. Eng.l* 1, 8-21.

Wu, D. 2003. Studies on novel heterocyclic compounds and their microbicidal efficacy. *Tetrahedron*. 59, 8649-8687.

List of figures

Figure 1: Dihydropyridine-based bioactive compounds

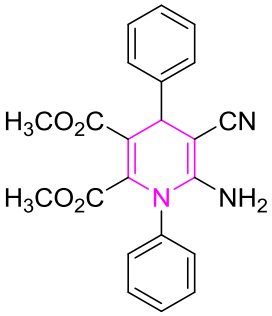

Anticancer Agent

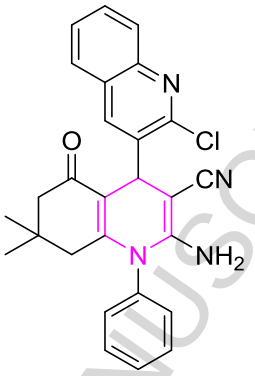

Antifungal Agent

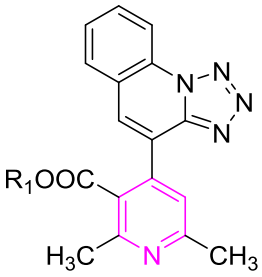

Anticancer Agent

Figure 2. Selected HMBC correlations for **A1**

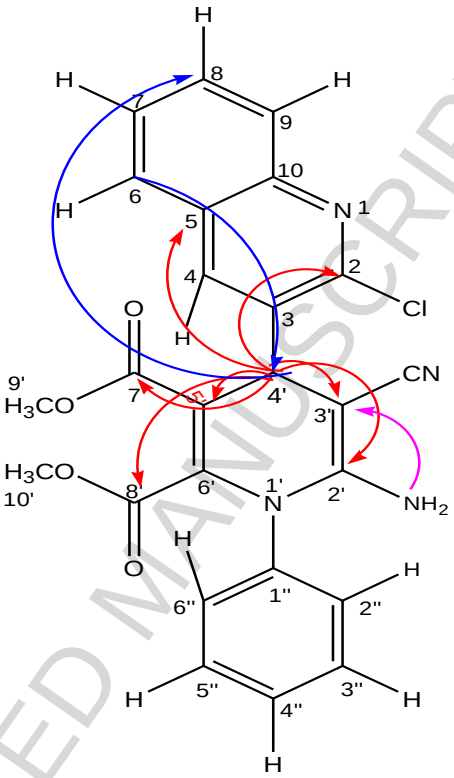

Figure 3. The cytotoxic effects of **A1** in the A549 lung cancer cell line

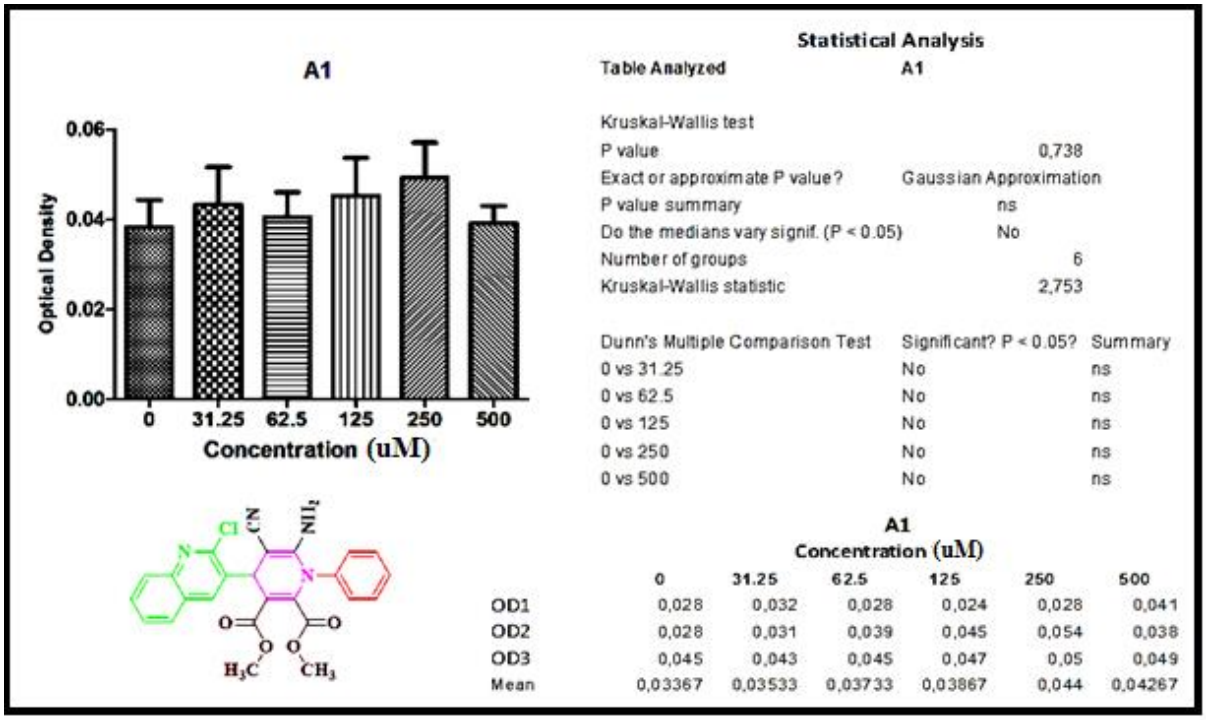

Statistical Analysis

Table Analyzed	A1
Kruskal-Wallis test	
P value	0,738
Exact or approximate P value?	Gaussian Approximation
P value summary	ns
Do the medians vary signif. (P < 0.05)	No
Number of groups	6
Kruskal-Wallis statistic	2,753

Dunn's Multiple Comparison Test	Significant? P < 0.05?	Summary
0 vs 31.25	No	ns
0 vs 62.5	No	ns
0 vs 125	No	ns
0 vs 250	No	ns
0 vs 500	No	ns

A1
Concentration (uM)

	0	31.25	62.5	125	250	500
OD1	0,028	0,032	0,028	0,024	0,028	0,041
OD2	0,028	0,031	0,039	0,045	0,054	0,038
OD3	0,045	0,043	0,045	0,047	0,05	0,049
Mean	0,03367	0,03533	0,03733	0,03867	0,044	0,04267

Figure 4. The cytotoxic effects of **A2** in the A549 lung cancer cell line

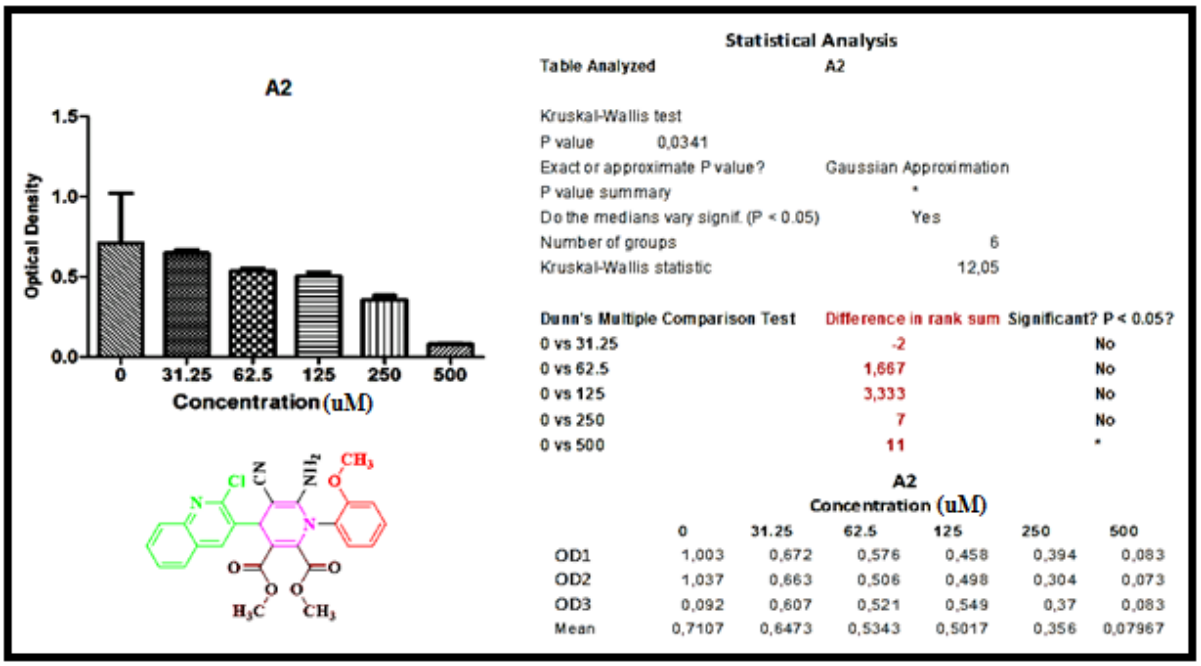

Statistical Analysis

Table Analyzed	A2
Kruskal-Wallis test	
P value	0,0341
Exact or approximate P value?	Gaussian Approximation
P value summary	*
Do the medians vary signif. (P < 0.05)	Yes
Number of groups	6
Kruskal-Wallis statistic	12,05

Dunn's Multiple Comparison Test	Difference in rank sum	Significant? P < 0.05?
0 vs 31.25	-2	No
0 vs 62.5	1,667	No
0 vs 125	3,333	No
0 vs 250	7	No
0 vs 500	11	*

A2
Concentration (uM)

	0	31.25	62.5	125	250	500
OD1	1,003	0,672	0,576	0,458	0,394	0,083
OD2	1,037	0,663	0,506	0,498	0,304	0,073
OD3	0,092	0,607	0,521	0,549	0,37	0,083
Mean	0,7107	0,6473	0,5343	0,5017	0,356	0,07967

Figure 5. The cytotoxic effects of **A3** in the A549 lung cancer cell line

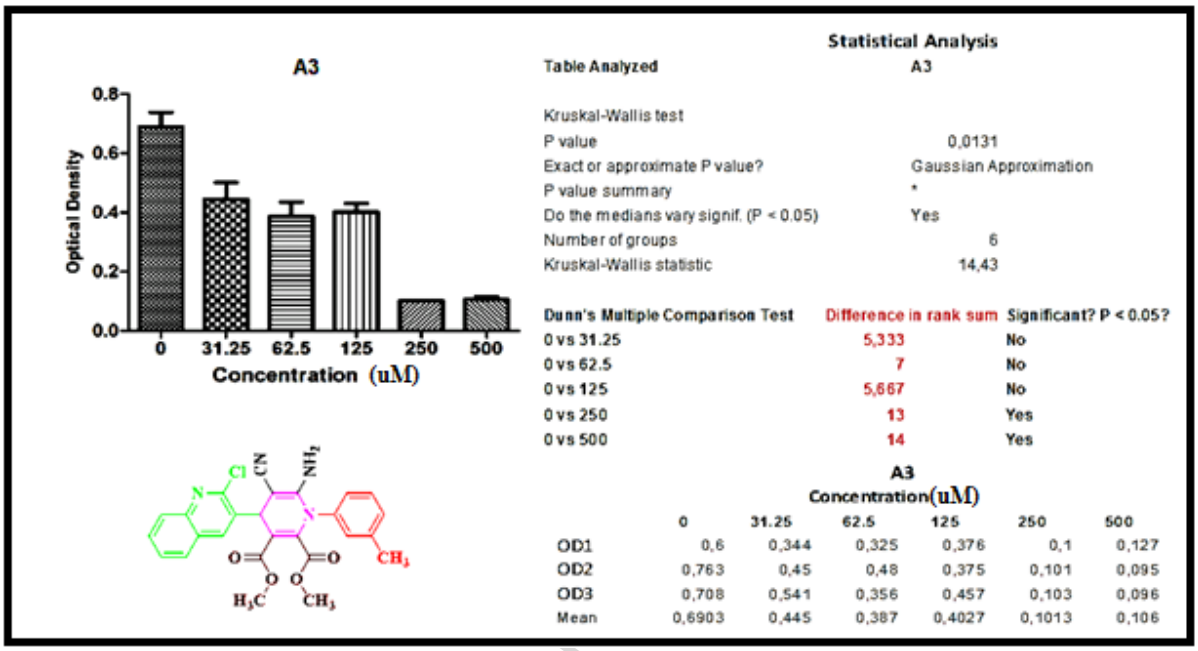

Statistical Analysis

Table Analyzed	A3
Kruskal-Wallis test	
P value	0,0131
Exact or approximate P value?	Gaussian Approximation
P value summary	*
Do the medians vary signif. (P < 0.05)	Yes
Number of groups	6
Kruskal-Wallis statistic	14,43

Dunn's Multiple Comparison Test	Difference in rank sum	Significant? P < 0.05?
0 vs 31.25	5,333	No
0 vs 62.5	7	No
0 vs 125	5,667	No
0 vs 250	13	Yes
0 vs 500	14	Yes

A3

Concentration(uM)

	0	31.25	62.5	125	250	500
OD1	0,6	0,344	0,325	0,376	0,1	0,127
OD2	0,763	0,45	0,48	0,375	0,101	0,095
OD3	0,708	0,541	0,356	0,457	0,103	0,096
Mean	0,6903	0,445	0,387	0,4027	0,1013	0,106

Figure 6. The cytotoxic effects of **A4** in the A549 lung cancer cell line

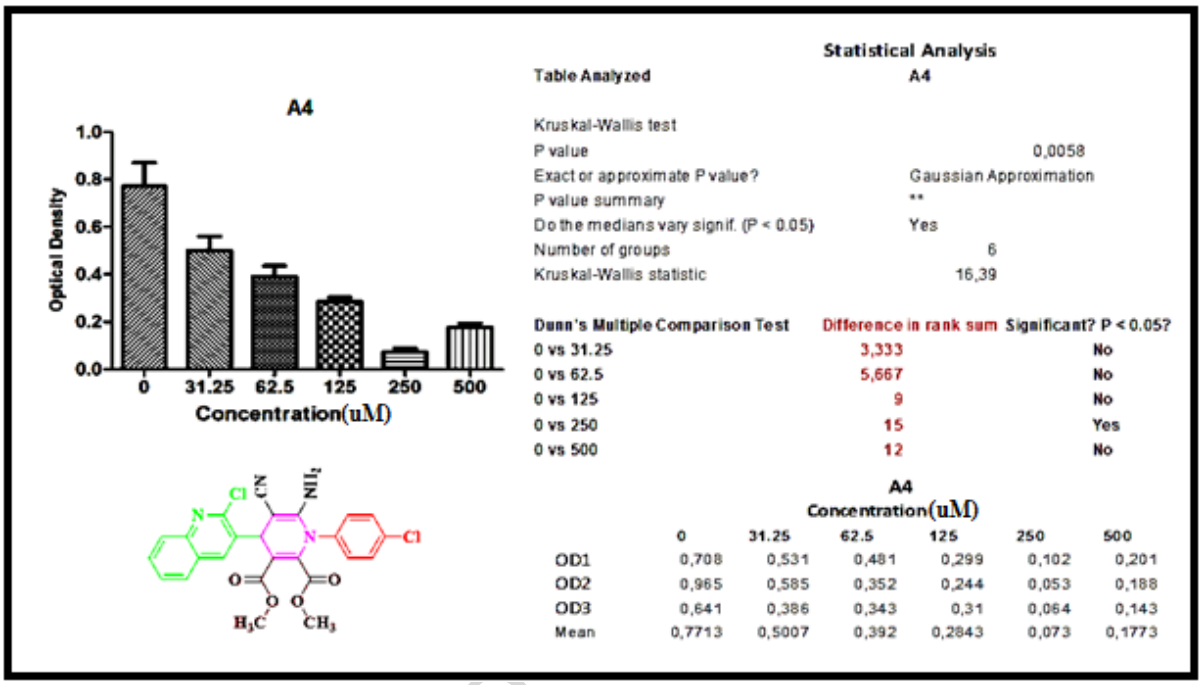

Statistical Analysis

Table Analyzed	A4
Kruskal-Wallis test	
P value	0,0058
Exact or approximate P value?	Gaussian Approximation
P value summary	**
Do the medians vary signif. (P < 0.05)	Yes
Number of groups	6
Kruskal-Wallis statistic	16,39

Dunn's Multiple Comparison Test	Difference in rank sum	Significant? P < 0.05?
0 vs 31.25	3,333	No
0 vs 62.5	5,667	No
0 vs 125	9	No
0 vs 250	15	Yes
0 vs 500	12	No

A4
Concentration(uM)

	0	31.25	62.5	125	250	500
OD1	0,708	0,531	0,481	0,299	0,102	0,201
OD2	0,965	0,585	0,352	0,244	0,053	0,188
OD3	0,641	0,386	0,343	0,31	0,064	0,143
Mean	0,7713	0,5007	0,392	0,2843	0,073	0,1773

Figure 7. The cytotoxic effects of **A5** in the A549 lung cancer cell line

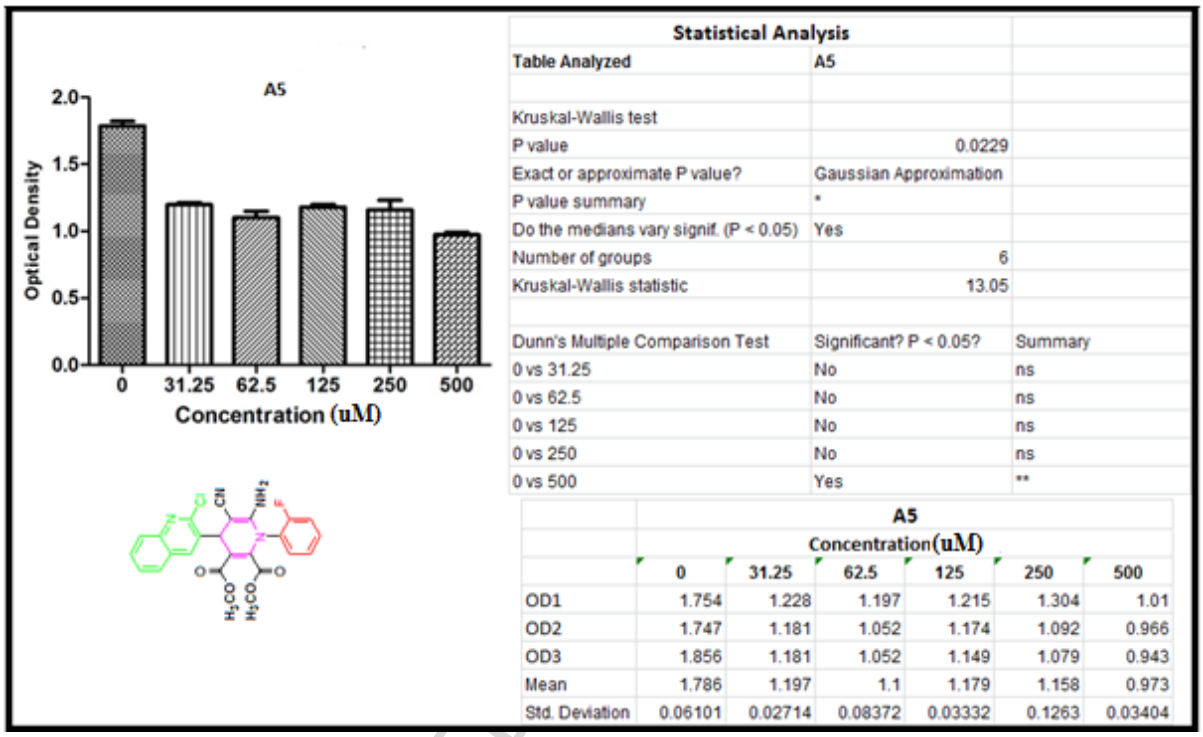

Statistical Analysis		
Table Analyzed	A5	
Kruskal-Wallis test		
P value	0.0229	
Exact or approximate P value?	Gaussian Approximation	
P value summary	*	
Do the medians vary signif. (P < 0.05)	Yes	
Number of groups	6	
Kruskal-Wallis statistic	13.05	
Dunn's Multiple Comparison Test	Significant? P < 0.05?	Summary
0 vs 31.25	No	ns
0 vs 62.5	No	ns
0 vs 125	No	ns
0 vs 250	No	ns
0 vs 500	Yes	**

	A5					
	Concentration(uM)					
	0	31.25	62.5	125	250	500
OD1	1.754	1.228	1.197	1.215	1.304	1.01
OD2	1.747	1.181	1.052	1.174	1.092	0.966
OD3	1.856	1.181	1.052	1.149	1.079	0.943
Mean	1.786	1.197	1.1	1.179	1.158	0.973
Std. Deviation	0.06101	0.02714	0.08372	0.03332	0.1263	0.03404

Figure 8. The cytotoxic effects of **A6** in the A549 lung cancer cell line

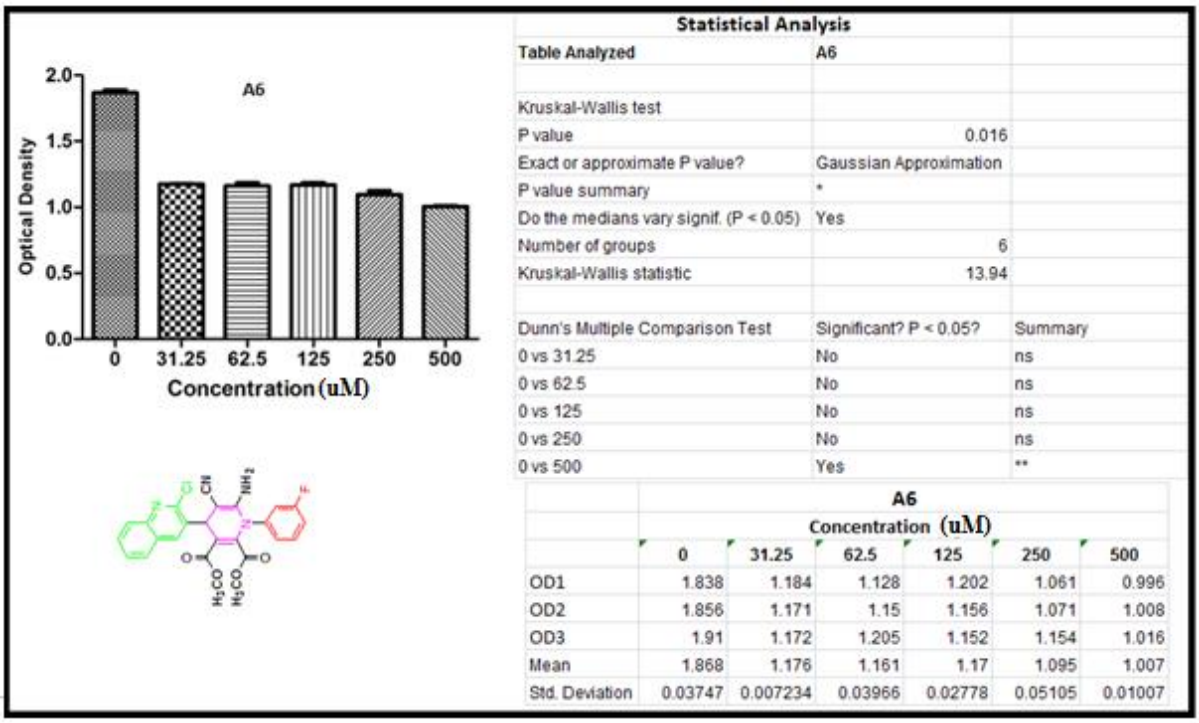

Statistical Analysis		
Table Analyzed	A6	
Kruskal-Wallis test		
P value	0.016	
Exact or approximate P value?	Gaussian Approximation	
P value summary	*	
Do the medians vary signif. (P < 0.05)	Yes	
Number of groups	6	
Kruskal-Wallis statistic	13.94	
Dunn's Multiple Comparison Test	Significant? P < 0.05?	Summary
0 vs 31.25	No	ns
0 vs 62.5	No	ns
0 vs 125	No	ns
0 vs 250	No	ns
0 vs 500	Yes	**

	A6					
	Concentration (uM)					
	0	31.25	62.5	125	250	500
OD1	1.838	1.184	1.128	1.202	1.061	0.996
OD2	1.856	1.171	1.15	1.156	1.071	1.008
OD3	1.91	1.172	1.205	1.152	1.154	1.016
Mean	1.868	1.176	1.161	1.17	1.095	1.007
Std. Deviation	0.03747	0.007234	0.03966	0.02778	0.05105	0.01007

Figure 9. The cytotoxic effects of **A7** in the A549 lung cancer cell line

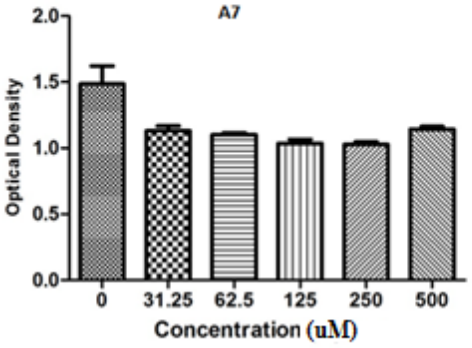

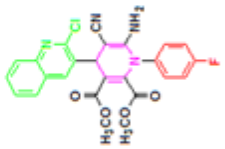

Statistical Analysis		
Table Analyzed	**A7**	
Kruskal-Wallis test		
P value	0.0176	
Exact or approximate P value?	Gaussian Approximation	
P value summary	*	
Do the medians vary signif. (P < 0.05)	Yes	
Number of groups	6	
Kruskal-Wallis statistic	13.7	
Dunn's Multiple Comparison Test	Significant? P < 0.05?	Summary
0 vs 31.25	No	ns
0 vs 62.5	No	ns
0 vs 125	No	ns
0 vs 250	Yes	*
0 vs 500	No	ns

	A7					
	Concentration (uM)					
	0	31.25	62.5	125	250	500
OD1	1.599	1.076	1.125	1.083	1.042	1.104
OD2	1.216	1.117	1.104	1.045	1.053	1.18
OD3	1.64	1.2	1.076	0.98	0.99	1.142
Mean	1.485	1.131	1.102	1.036	1.028	1.142
Std. Deviation	0.2339	0.06317	0.02458	0.05209	0.03365	0.038

Figure 10. The cytotoxic effects of **A8** in the A549 lung cancer cell line

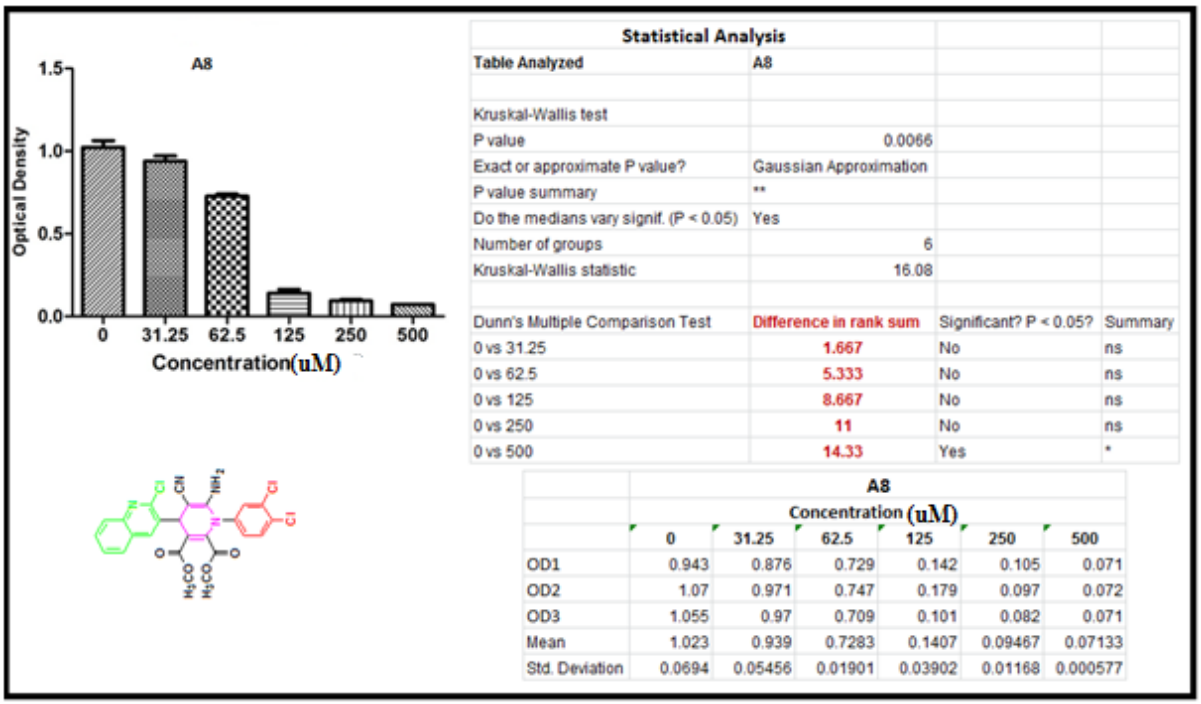

Statistical Analysis			
Table Analyzed	A8		
Kruskal-Wallis test			
P value	0.0066		
Exact or approximate P value?	Gaussian Approximation		
P value summary	**		
Do the medians vary signif. (P < 0.05)	Yes		
Number of groups	6		
Kruskal-Wallis statistic	16.08		
Dunn's Multiple Comparison Test	Difference in rank sum	Significant? P < 0.05?	Summary
0 vs 31.25	1.667	No	ns
0 vs 62.5	5.333	No	ns
0 vs 125	8.667	No	ns
0 vs 250	11	No	ns
0 vs 500	14.33	Yes	*

	A8					
	Concentration (uM)					
	0	31.25	62.5	125	250	500
OD1	0.943	0.876	0.729	0.142	0.105	0.071
OD2	1.07	0.971	0.747	0.179	0.097	0.072
OD3	1.055	0.97	0.709	0.101	0.082	0.071
Mean	1.023	0.939	0.7283	0.1407	0.09467	0.07133
Std. Deviation	0.0694	0.05456	0.01901	0.03902	0.01168	0.000577

Figure 11a, 11b & 11c. Molecular docking result of **A1** with human mdm2

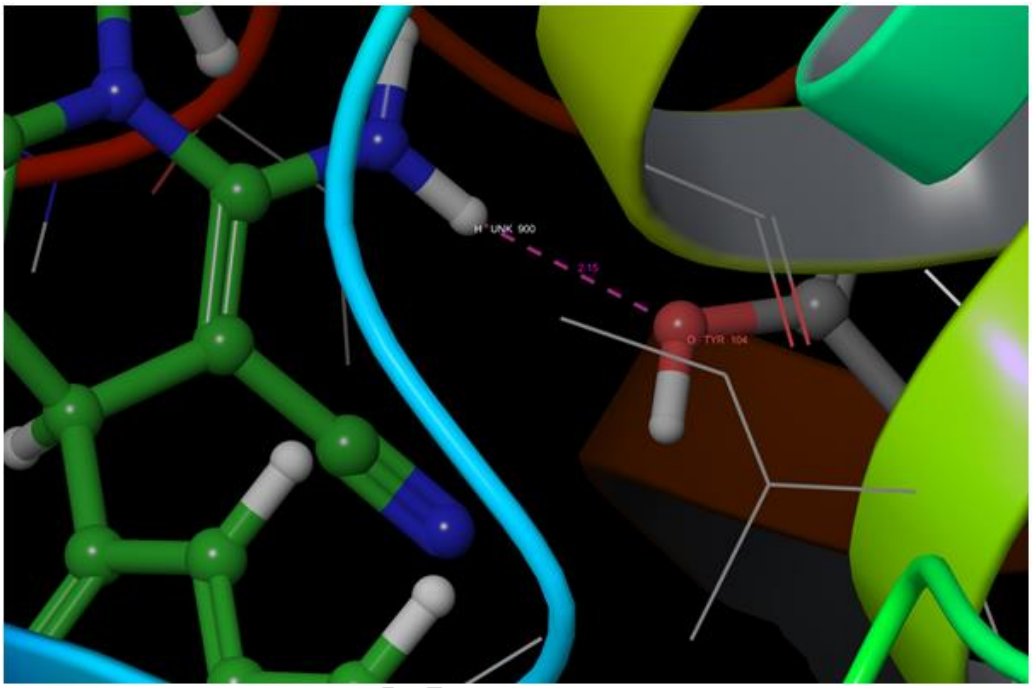

Figure 11a.

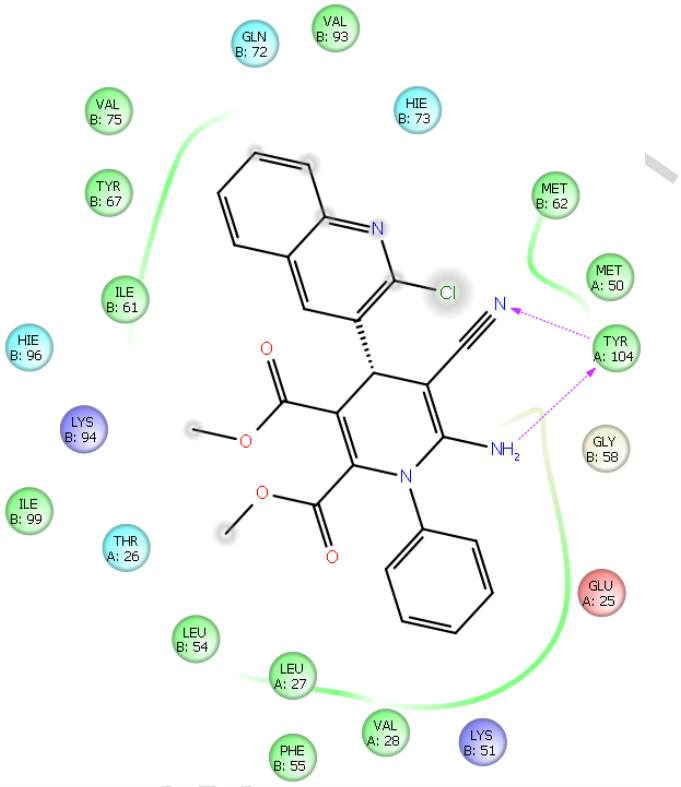

Figure 11b.

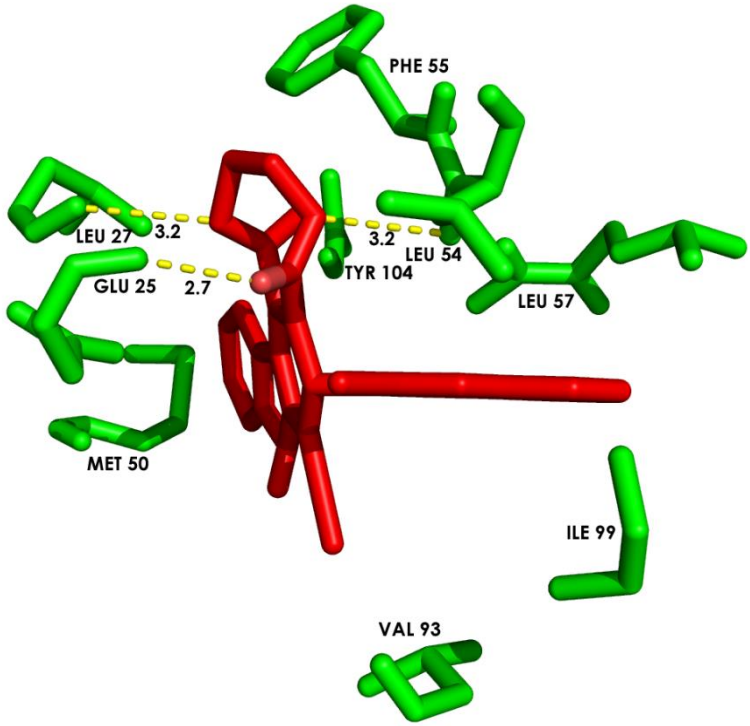

Figure 11c.

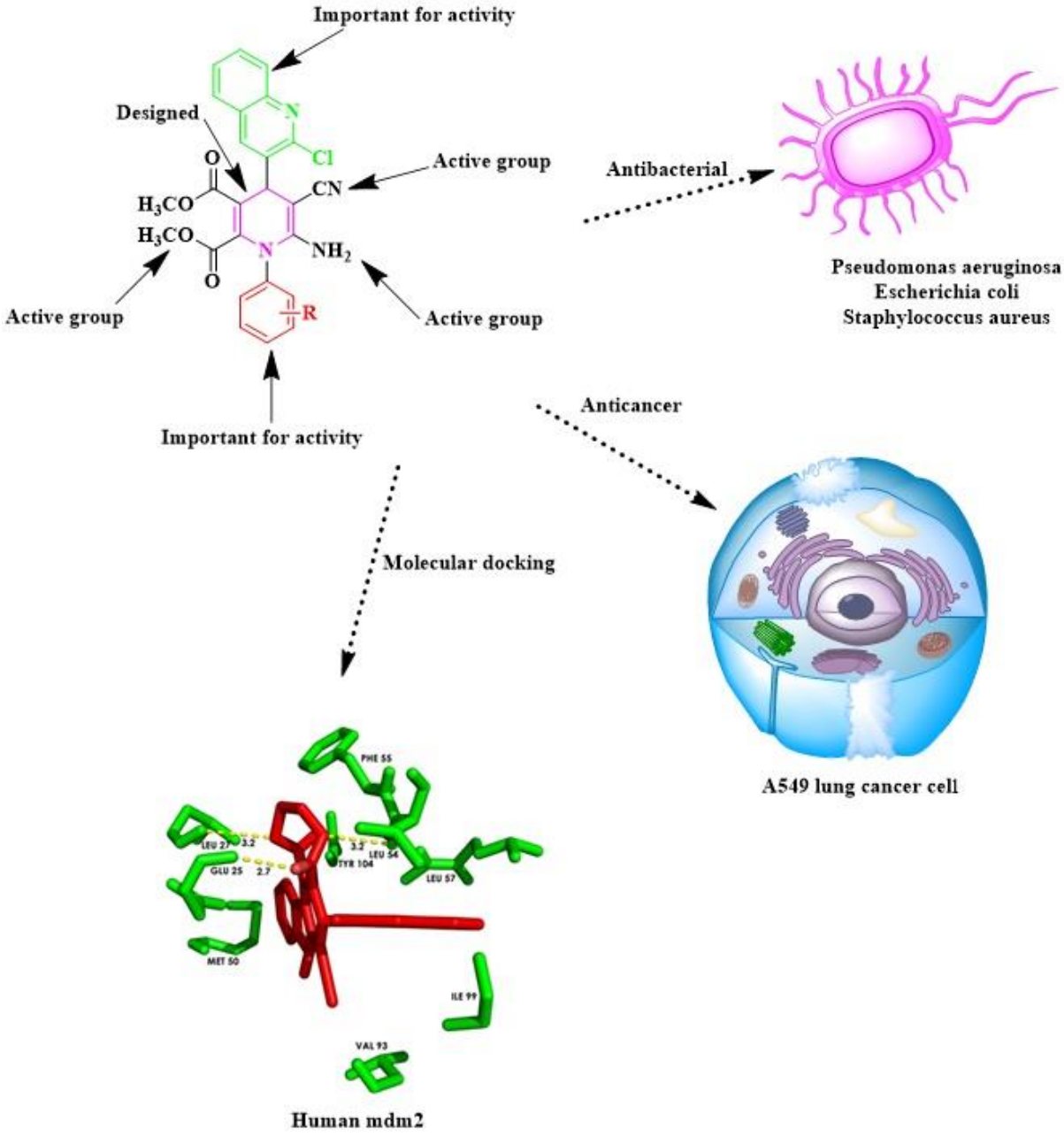

Graphical abstract

Highlights

- A new series of quinoline derivatives **A1-A8 synthesis via one pot reaction**
- All compounds characterized by FTIR, NMR (^{1}H, ^{13}C, ^{19}F, 2D NMR), HRMS
- All compounds identified as potent anticancer and antibacterial agent
- Better inhibitor for E3 ubiquitin-protein ligase mdm2